J. Fluid Mech. (2006), *vol.* 548, *pp.* 133–140.
doi:10.1017/S0022112005007664 Printed in the United Kingdom

Rise speed of supercritical carbon dioxide spheres in aqueous surfactant solutions

By SHIGERU BANDO[1] AND FUMIO TAKEMURA[2]

[1]Department of Mechanical Engineering, The University of Tokyo, 7-3-1 Hongo, Bunkyo, Tokyo 113-8656, Japan

[2]National Institute of Advanced Industrial Science and Technology 1-2-1 Namiki, Tsukuba, Ibaraki 305-8564, Japan

(Received 23 May 2005 and in revised form 14 October 2005)

The rise speed of supercritical carbon dioxide spheres in aqueous surfactant solution was investigated experimentally. Decanonic acid was added to water as a surfactant, and then the rise speed of the CO_2 spheres was measured at pressures 5 MPa to 10 MPa and at temperatures 28 °C to 40 °C generating different phases of spheres, namely gas, liquid, and supercritical. The results revealed that gas bubbles and liquid droplets showed the same behaviour as a rising rigid sphere due to the adsorption of surfactant onto the surface of the spheres. In contrast, due to the absorption of surfactant into the spheres, the drag coefficient of spheres of supercritical fluid was lower than that of a rigid sphere and was similar to that of a fluid sphere with a moving boundary. This behaviour mainly occurred in the rising process of the spheres composed of supercritical CO_2.

1. Introduction

In water that contains surfactant, the drag force on a bubble increases due to adsorption of the surfactant (see Cuenot, Magnaudet & Spennato 1997; Zhang & Finch 2001; Liao & McLaughlin 2000), although bubbles have a shear-free boundary in 'hyper clean' water (Duinveld 1995). The drag force continues to increase until the bubbles behave like rigid spheres (see Clift, Grace & Weber 1978; Karamanev 1994). The mechanism responsible for this behaviour was experimentally studied by Savic (1953) and is known as the 'stagnant cap model'. Cuenot *et al.* (1997) numerically studied both the diffusion of surfactants in the bulk and the adsorption–desorption process of surfactants onto the surface of a bubble, and precisely analysed the transient mechanism of the bubble behaviour. They concluded that a surface tension distribution is formed due to adsorption of surfactant, and that this distribution causes the formation of a no-slip boundary. A stagnant cap is also formed at the liquid droplet surface when the droplet moves in water that contains surfactant (see Garner & Skelland 1955; Elzinga & Banchero 1961). As the stagnant cap grows from the back side of the droplet, the centre of the vortex formed inside the droplet shifts forward (Horton, Fritsch & Kintner 1965; Huang & Kintner 1969; Oguz & Sadhal 1988) and finally the droplet behaves like a rigid sphere.

Supercritical CO_2 is defined as non-condensable fluid that is above critical temperature (31.05 °C) and pressure (7.39 MPa). Although gases at low pressure have no ability to absorb organic materials, including surfactants, supercritical CO_2 has this absorption ability is therefore used as a solvent in certain extraction processes

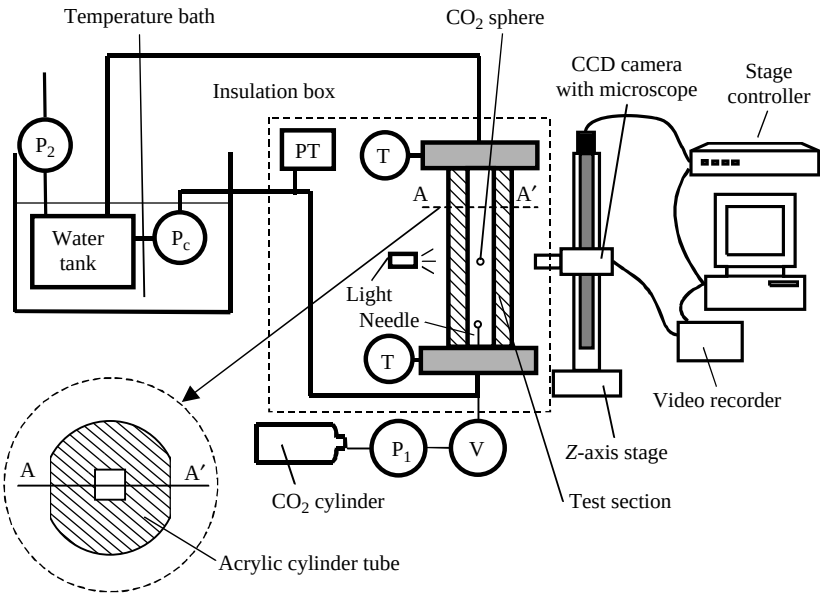

FIGURE 1. Schematic of experimental setup to measure radius and rise speed of spheres.

(see Sang-Do & Akgerman 1990). In contrast, liquids lose the ability to absorb surfactants because the diffusivity of material decreases in the liquid phase. Therefore, spheres composed of supercritical fluids might show different behaviour from bubbles and liquid droplets because such spheres can absorb certain surfactants and no stagnant cap might be formed at the surface.

In this study, the effect of absorption ability on the change of surface concentration of surfactants is clarified. First, the rise speed of CO_2 spheres in water that contained surfactant was measured at pressures 5 MPa to 10 MPa and at temperatures 28 °C to 40 °C generating different phases of spheres, namely gas, liquid, and supercritical. The results revealed that the drag coefficients of gas bubbles and liquid droplets were the same as that of a rigid sphere, whereas that of spheres of supercritical fluid was lower than that of a rigid sphere and similar to that of a fluid sphere with a moving boundary. Then, the conditions at which this behaviour changed from that of a rigid sphere to a fluid sphere were measured, and the changes were plotted on a calculated pressure–enthalpy diagram of CO_2.

2. Experimental setup and procedure

Figure 1 shows a schematic of the experimental setup used to measure the radius and rise speed of the spheres. It consists of a test section, a needle to produce single CO_2 spheres, a water storage tank and temperature bath to control the temperature of the water, an insulation box to maintain the temperature of the test section, a pressure transducer to measure the system pressure (TEAC Co., TP-AP 20 MPa), two syringe pumps to pressurize the carbon dioxide and water, P_1 and P_2 respectively (GL Science, PU610A-00 and MP680), a circulation pump, P_c (Akico Co.), a valve, V_1, and a system to measure the radius and rise speed of the spheres. The measurement system consists of a z-axis stage, stage controller, CCD camera with a microscope, light source, video recorder, and a video capture board and PC to control the system. The

	Exp. 1	Exp. 2	Exp. 3	Exp. 4	Exp. 5
Temperature (°C)	29.6	28.9	33.5	34.5	33.8
Pressure (MPa)	5.7	8.4	7.6	9.2	7.3
Phase of CO_2	Gas	Liquid	Supercritical	Supercritical	Supercritical
Initial radius R_i (mm)	0.232	0.367	0.207	0.23	0.28
Density of CO_2 ($kg\,m^{-3}$)	155.96	738.55	337.78	684.57	260.30
Density of H_2O ($kg\,m^{-3}$)	998.22	999.65	997.85	998.20	997.61
Viscosity of CO_2 (μPa s)	17.53	61.07	28.77	54.05	21.29
Viscosity of H_2O (μPa s)	801.94	815.48	741.30	726.64	736.84

TABLE 1. Experimental conditions for measuring rise speed of spheres.

test section was a 420 mm long acrylic cylinder tube with a 15×15 mm inner square cross-section and a 100 mm outer diameter. To accurately clarify the mechanism of mass transfer of surfactant, the rise velocity of spheres must be measured without shrinking the spheres. Measuring the rise speed in aqueous solution saturated with CO_2 is difficult using this experimental apparatus, however, because acrylic does not have CO_2 resistance. To avoid distortion of the spheres due to the curvature of the cylinder surface, the outside of the cylinder was shaved as shown in cross-section A-A′. The needle to produce CO_2 spheres was made from a PEEKsil tube (Upchurch Co., 3255) with a 25 μm inner diameter. This tube has a good wettability surface that stably produces single spheres with diameters less than 1.0 mm. The needle was connected to the syringe pump (P_1). The diameter of the spheres was controlled by regulating the opening angle (V_1). The CCD camera had a resolution of 640×480 pixels and each pixel corresponded to about 2.5 μm through the microscope. The CCD camera with the microscope was fixed to the Z-axis stage and used to track the rising spheres. The system used to control the camera speed has been described previously (Takemura & Yabe 1999). The water was purified using a water purification system (MILLIPORE, Milli-Q) and the specific resistance of the water was 18.2 MΩ cm. Decanonic acid was added to $0.05\,mol\,m^{-3}$ as a surfactant. Because its molecular weight ($=172\,g\,mol^{-1}$) is relatively heavy as a surfactant and because its desorption rate is small, bubbles or droplets behave like rigid spheres at low concentration ($<0.05\,mol\,m^{-3}$) and at a viscosity of the solution the same as water. For example, according to the calculation by Cuenot *et al.* (1997), the drag of a 1.0 mm diameter bubble reaches that of a rigid sphere within 0.5 s in $0.01\,mol\,m^{-3}$ decanonic acid solution. Because a $0.05\,mol\,m^{-3}$ decanonic acid solution was used in our experiments, the surfactant had adsorbed onto the surface of the sphere at the beginning of the rising process. Table 1 lists the experimental conditions.

Considering the balance between buoyancy and drag forces acting on a sphere, the drag coefficient of spheres at steady state can be expressed as

$$C_D = \frac{8(\rho_w - \rho_{CO_2})Rg}{3\rho_w U^2} \tag{1}$$

where R is the radius of the sphere, U is the rise speed of the sphere, ρ_w is the density of water, ρ_{CO_2} is the density of CO_2, and g is the gravitational constant. The drag coefficient of a rigid sphere rising in an infinite liquid is expressed as (Clift *et al.* 1978)

$$C_{D,S} = \frac{24}{Re}(1 + 0.15\,Re^{0.687}) \tag{2}$$

where Reynolds number (Re) is defined as $2RU/\nu_w$, and ν_w is the kinematic viscosity of water. Based on comparisons between numerical results and several predictive equations, Oliver & Chung (1987) recommended the following predictive equation for expressing the drag coefficient of a fluid sphere:

$$C_{D,F} = \frac{1}{1+\kappa}\left[\kappa\left(\frac{24}{Re} + 4\,Re^{-1/3}\right) + 14.9Re^{-0.78}\right] \tag{3}$$

where κ denotes μ_{CO_2}/μ_w, and μ_{CO_2} and μ_w are viscosities of CO_2 and water, respectively.

In this study, the experimental results were compared with the two steady solutions in equations (2) and (3). In our experiments, the wall effect and the unsteady terms (e.g. acceleration of the spheres, added mass force, and history force) can be neglected. When the ratio of the sphere diameter ($2R$) to the width of the cross-section of a flow field is less than 0.06, the wall effect on the rise speed is negligible (Clift *et al.* 1978). Because spheres of $2R < 0.8$ mm rise in a 15×15 mm cross-section where this ratio is 0.053, the wall effect can be neglected. Considering the change in R with time, the ratios of the acceleration (α_1) and added mass force (α_2) to the buoyancy force in the rising process (Magnaudet & Eames 2000) are expressed as

$$\left.\begin{aligned} \alpha_1 &= \frac{\rho_{CO_2}}{(\rho_w - \rho_{CO_2})g}\frac{dU}{dt}, \\ \alpha_2 &= \frac{1}{2}\frac{\rho_w}{(\rho_w - \rho_{CO_2})g}\frac{dU}{dt} + \frac{3}{2}\frac{\rho_w U}{(\rho_w - \rho_{CO_2})Rg}\frac{dR}{dt}. \end{aligned}\right\} \tag{4}$$

Because the maximum α_1 and α_2 calculated from our experimental values are $O(10^{-4})$ and $O(10^{-3})$, respectively, both the acceleration of the spheres and the added mass force can also be neglected in the rising process. The history force on the spheres should be considered when the ratio of the rate of change in R to U is greater than 1 (Magnaudet & Legendre 1998). For example, Takemura & Magnaudet (2004) showed that the history force reached half that of the buoyancy force in a rapid dissolution process of a CO_2 bubble in a 2 mol l^{-1} sodium hydroxide solution. In their experiments, the ratio of the change in R to U was $O(10^{-1})$. In our experiments, because the maximum value of this ratio was $O(10^{-3})$, the history force could be neglected.

3. Results and discussion

Figure 2 shows the time evolution of R normalized by the initial radius R_i (table 1). R decreased as the CO_2 dissolved into the water. Figure 3 shows the time evolution of U, clearly showing that U decreased as the spheres decreased in size. Figure 4 shows the time evolution of C_D normalized as follows:

$$C_D^* = \frac{C_D - C_{D,F}}{C_{D,S} - C_{D,F}}. \tag{5}$$

Based on figure 4, a CO_2 gas bubble and a CO_2 liquid droplet exhibit the same C_D^* as a rigid sphere at the beginning of the rising process, and this C_D^* remains constant even during the decrease in R due to the dissolution of CO_2 into water. In contrast, although the supercritical CO_2 spheres under two conditions (Exp. 4 and Exp. 5) initially exhibited the same C_D^* as a rigid sphere, their C_D^* approached that of a fluid sphere with a moving boundary with time and this shows that the surface remobilizes.

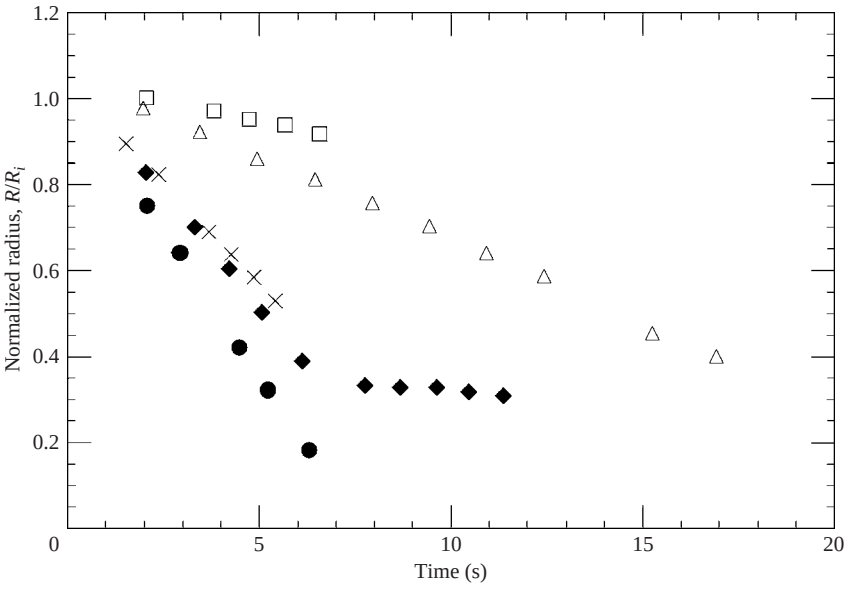

FIGURE 2. Time evolution of sphere radius R normalized by initial radius R_i. ●, Gas (Exp. 1), □; Liquid (Exp. 2), ◆; Supercritical (Exp. 3); △, Supercritical (Exp. 4); ×, Supercritical (Exp. 5).

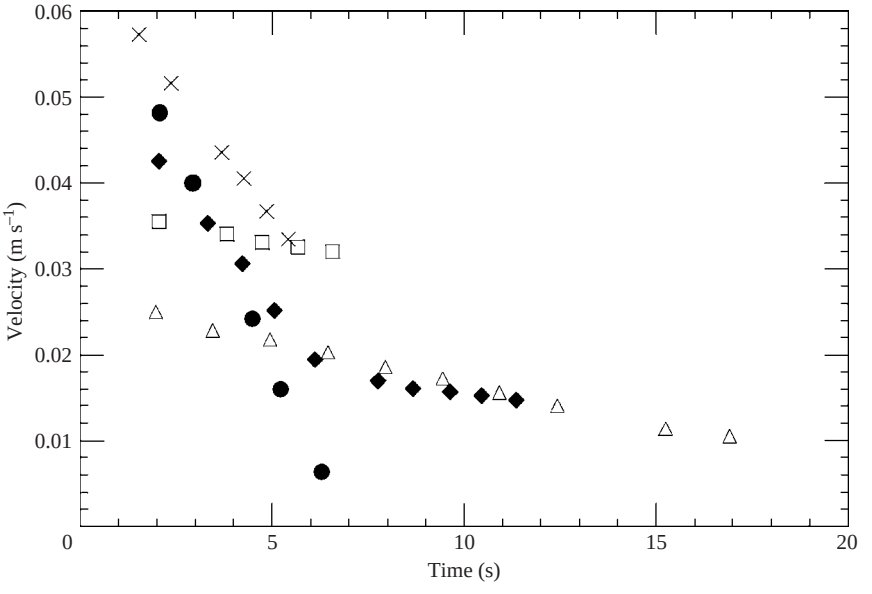

FIGURE 3. Time evolution of sphere velocity U. Symbols as figure 2.

The supercritical CO_2 spheres under the conditions for Exp. 3 initially exhibited a C_D^* smaller than that of a rigid sphere, and finally, C_D^* approached 0. During the rising process, because the surface area of spheres monotonically decreases, the surface concentration of surfactant does not decrease unless the surfactant is absorbed into the spheres. Additionally, in the experimental conditions studied here, the properties of water remained relatively constant, whereas those of CO_2 changed significantly

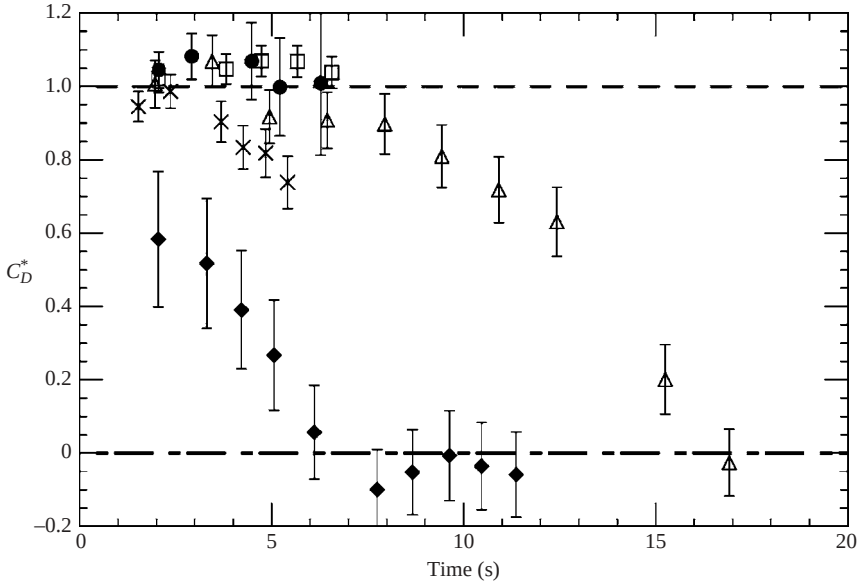

FIGURE 4. Time evolution of normalized drag coefficient C_D^*. Symbols as figure 2.

(table 1). Therefore the decrease in C_D^* in our experiment must indicates the absorption of the surfactant into the supercritical CO_2 spheres, which in turn decreases the surface concentration of the surfactant. Because solubility of decanonic acid in supercritical CO_2 at 40 °C is 0.178 in mole fraction at 10.3 MPa and is 0.306 at 7.54 MPa (Heo *et al.* 2001), a 0.5 mm diameter supercritical CO_2 sphere can absorb 1.5×10^{-7} mol decanonic acid at 40 °C and 7.54 MPa. Assuming that the boundary layer of a rising 0.5 mm diameter supercritical CO_2 sphere is twice the diameter of the sphere itself, the sphere can encounter a maximum of 1.5×10^{-8} mol of decanonic acid. This concentration is not sufficient for the sphere to be saturated with decanonic acid, nor can the sphere absorb all the decanonic acid it encounters. Although the surfactant was sufficiently adsorbed onto the surface of the spheres at rest (i.e. not rising or descending) due to the slow absorption process of the surfactant into the spheres, the absorption rate increases with the development of the circulation inside the spheres during the rising process, and thus the surface concentration decreases.

Although C_D^* of the supercritical CO_2 spheres decreased under the three experimental conditions studied here (table 1), the rate of decrease differed for the three conditions. This difference is assumed to be caused by differences in pressure, temperature, and thermophysical properties, such as the solubility and diffusivity of decanonic acid in supercritical CO_2. Because quantitative numerical analysis of the transport process of decanonic acid onto the surface of a CO_2 sphere from the bulk and into the sphere itself is difficult due to the lack of information about the thermophysical properties, in this study we only investigated the condition in which C_D of supercritical CO_2 spheres decreases. Figure 5 shows the experimental change in C_D from that of a rigid sphere, plotted on the calculated pressure–enthalpy diagram of CO_2. If $C_D^* < 0.8$, then C_D^* of the CO_2 spheres was considered to have decreased (●) with respect to C_D^* of rigid spheres, and if $C_D^* > 0.8$, then it was considered to have remained similar (×) to that of rigid spheres. (The measured C_D plotted in the figure was that measured at the top of the test section.) The figure shows

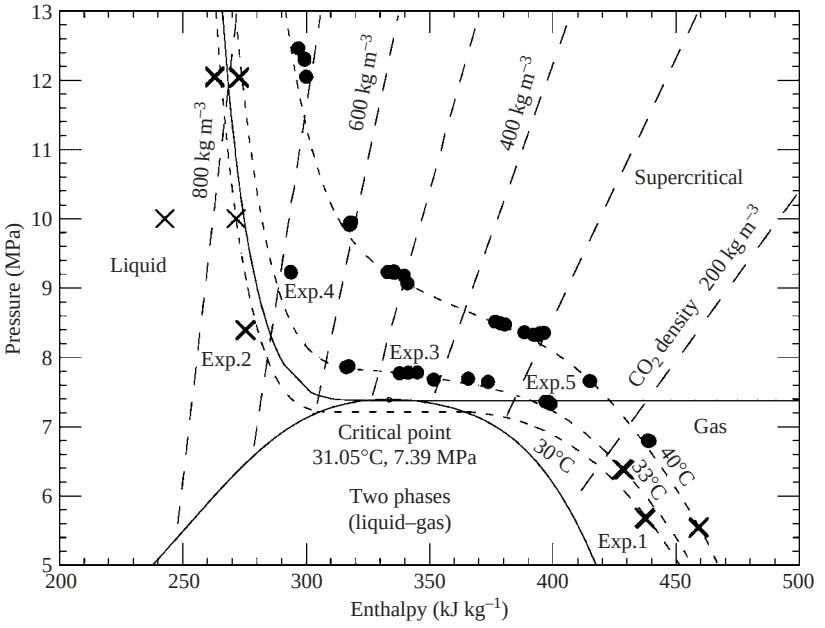

FIGURE 5. Experimental change in C_D of supercritical CO_2 spheres from that of a rigid sphere plotted on a calculated pressure–enthalpy diagram of CO_2. ●, Condition where the value of C_D^* decreased less than 0.8. (Exp. 3, 4, 5). ×, Condition where the value of C_D^* increased more than 0.8. (Exp. 1, 2).

that the behaviour of the supercritical CO_2 spheres clearly differed from that of CO_2 gas bubbles and CO_2 liquid droplets. In general, compared to that of a rigid sphere, C_D^* of the gas bubbles and liquid droplets was similar, whereas that of the supercritical CO_2 spheres was lower. The spheres with CO_2 density between 200 and 700 kg m^{-3} showed a decrease in C_D^* with respect to C_D^* of a rigid sphere. Stebe, Lin & Maldarelli (1991) explained that remobilization is caused if, relative to the rate of surface convection, (i) the surfactant has fast desorption kinetics, and (ii) the surfactant is present in bulk concentrations high enough so that diffusive boundary layers are depressed, and (iii) the rate of bulk diffusion becomes fast. In our case the remobilization of a large sphere at the beginning of the rise process might be explained by the first mechanism because the concentration in the sphere is low. During the sphere shrinking, surfactant continuously dissolves into the sphere and the surfactant concentration increases; nevertheless the value of C_D^* is the same that of a fluid sphere. In this stage, the remobilization might be explained by the second mechanism. When the relative amounts of water, CO_2 and surfactant is changed, the solubility of CO_2 possibly becomes low near the surface. This might be the reason why the shrinking rate of sphere suddenly decreases as shown in figure 3.

The supercritical CO_2 spheres at different conditions (table 1) showed different rates of changes in C_D^* (figure 4), and the gradient of this change for conditions in Exp. 3 was higher than that in Exps. 4 and 5. In the pressure–enthalpy diagram (figure 5), the conditions for Exp. 4 were closer to the liquid phase than were those for Exp. 3, and the conditions for Exp. 5 were closer to the gas phase than were those for Exp. 3. The gradient might be high at the centre of the supercritical region, and then low when the fluid conditions approach the gas or liquid phase.

REFERENCES

Clift, R., Grace, J. R. & Weber, M. E. 1978 *Bubbles, Drops and Particles*. pp. 30–279. Academic.

Cuenot, B., Magnaudet, J. & Spennato, B. 1997 The effects of slightly soluble surfactants on the flow around a spherical bubble. *J. Fluid Mech.* **339**, 25–53.

Duineveld, P. C. 1995 The rise velocity and shape of bubbles in pure water at high Reynolds number. *J. Fluid Mech.* **292**, 325–332.

Elzinga, E. R. & Banchero, J. T. 1961 Some observations on the mechanics of drops in liquid-liquid systems. *AIChE J.* **7**, 394–399.

Garner, F. H. & Skelland, A. H. D. 1955 Some factors affecting droplet behaviour in liquid-liquid systems. *Chem. Engng Sci.* **4**, 149–158.

Griffith, R. M. 1962 The effect of surfactants on the terminal velocity of drops and bubbles. *Chem. Engng Sci.* **17**, 1057–1070.

Heo, J. H., Shin, H. Y., Park, J. U., Joung, S. N., Kim, S. Y. & Yoo, K. P. 2001 Vapor-liquid equilibria for binary mixtures of CO_2 with 2-methyl-2-butanol, octanoic acid, decanonic acid at temperature from 313.15 K to 353.15 K and pressures from 3 MPa to 24 MPa. *J. Chem. Engng Data* **46**, 355–358.

Horton, T. J., Fritsch, T. R. & Kintner, R. C. 1965 Experimental determination of circulation velocities inside drops. *Can. J. Chem. Engng* **43**, 143–146.

Huang, W. S. & Kintner, R. C. 1969 Effects of surfactants on mass transfer inside drops. *AIChE J.* **15**, 735–744.

Karamanev, D. G. 1994 Rise of gas bubbles in quiescent liquids. *AIChE J.* **40**, 1418–1421.

Liao, Y. & McLaughlin, J. B. 2000 Bubble motion in aqueous surfactant solutions. *J. Colloid Interface Sci.* **224**, 297–310.

Magnaudet, J. & Eames, I. 2000 The motion of high-Reynolds-number bubbles in inhomogeneous flows. *Annu. Rev. Fluid Mech.* **32**, 659–708.

Magnaudet, J. & Legendre, D. 1998 The viscous drag force on a spherical bubble with a time-dependent radius. *Phys. Fluids* **10**, 550–554.

Oguz, H. N. & Sadhal, S. S. 1988 Effects of soluble and insoluble surfactants on the motion of drops. *J. Fluid Mech.* **194**, 563–579.

Oliver, D. L. R. & Chung, J. N. 1987 Flow about a fluid sphere at low to moderate Reynolds number. *J. Fluid Mech.* **177**, 1–18.

Sang-Do, Yeo. & Akgerman, A. 1990 Supercritical extraction of organic mixtures from aqueous solutions, *AIChE J.* **36**, 1743–1747.

Savic, P. 1953 Circulation and distortion of liquid drops falling through a viscous medium. *Tech. Rep.* MT-22. Natl Res. Counc. Can., Div. Mech. Engng.

Stebe, K. J., Lin, S. Y. & Maldarelli, C. 1991 Remobilizing surfactant retarded fluid particle interfaces. I. Stress-free conditions at the interfaces of micellar solutions of surfactants with fast sorption kinetics. *Phys. Fluids* A **3**, 3–20.

Takemura, F. & Magnaudet, J. 2004 The history force on a rapidly shrinking bubble rising at finite Reynolds number. *Phys. Fluids* **16**, 3247–3255.

Takemura, F. & Yabe, A. 1998 Gas dissolution process of spherical rising gas bubbles. *Chem. Engng Sci.* **53**, 2691–2699.

Zhang, Y. & Finch, J. A. 2001 A note on single bubble motion in surfactant solutions. *J. Fluid Mech.* **429**, 63–66.